Int. J. Heat Mass Transfer. Vol. 19, pp. 1441–1453. Pergamon Press 1976. Printed in Great Britain

BUBBLE INDUCED HEAT TRANSFER IN GAS FLUIDIZED BEDS

J. KUBIE*
Department of Mechanical Engineering, University of Aston in Birmingham, England

(*Received* 3 *February* 1975 *and in revised form* 29 *March* 1976)

Abstract—The influence of gas bubbles on heat transfer in gas fluidized beds has been investigated. A platinum wire has been used as a heat-transfer probe and the aggregative gas fluidized bed has been simplified by generating a single continuous stream of gas bubbles into an incipiently fluidized bed. It has been found that in the case of aggregative gas fluidized beds of small particles operating below the radiative temperature level, transient conduction into the emulsion phase is responsible for at least 90% of heat transfer and that the remainder is contributed by the superimposed gas convection. A theoretical model of the bubble induced heat transfer has been developed. Finally, experimental justification for the concept of the property boundary layer introduced in [2] is presented.

NOMENCLATURE

a, wire radius [m];
a_P, particle radius [m];
c_P, specific heat [J/kg K];
$c_P(r)$, specific heat of emulsion at point r [J/kg K];
f, frequency of bubble generation [1/s];
$fn(x)$, function of x;
Fo, $(\kappa_E t/a^2)$, instantaneous Fourier number;
Fo_m, (κ_E/fa^2), time-mean Fourier number;
k, thermal conductivity [W/m K];
$k(r)$, thermal conductivity of emulsion at point r [W/m K];
L, wire halflength [m];
Nu, Qa^2/Tk_E, theoretically calculated Nusselt number;
Nu_x, $Qa^2/\Delta Tk_E$, experimentally obtained Nusselt number;
Q, heat generation per unit volume of the wire [W/m^3];
r, space coordinate [m];
Δr, $r-a$, distance from the wire surface [m];
t, time [s];
T, space average wire temperature [K];
T_E, emulsion temperature [K];
T_{E1}, first approximation to the emulsion temperature [K];
T_{E2}, emulsion temperature due to non-zero initial wire temperature [K];
T_0, initial wire temperature [K];
T_{0A}, initial space-average wire temperature [K];
T_W, wire temperature [K];
T_{W1}, first approximation to the wire temperature [K];
T_{W2}, wire temperature due to non-zero initial wire temperature [K];
T_X, experimentally obtained average wire temperature [K];
T_∞, bed temperature [K];
ΔT, $T_X - T_\infty$, temperature difference [K];
U, superficial gas velocity [m/s];
U_{mf}, minimum fluidizing velocity [m/s];
x, space coordinate [m].

Greek symbols

ε, voidage;
$\varepsilon(r)$, emulsion voidage at point r;
κ, thermal diffusivity [m^2/s];
$\kappa(r)$, thermal diffusivity of emulsion at point r [m^2/s];
ρ, specific density [kg/m^3];
$\rho(r)$, specific density of emulsion at point r [kg/m^3];
τ, $1/f$, periodic time [s];
τ_b, bubble residence time on the wire surface [s].

Subscripts

1, first approximation to;
2, due to the non-zero initial wire temperature;
c, corrected;
E, emulsion;
i, instantaneous;
m, time-mean;
P, particle;
W, wire.

1. INTRODUCTION

AN AGGREGATIVE gas fluidized bed contains regions of low (and sometimes zero) solid density which are called gas bubbles and a region of higher solid density which is called emulsion phase (or emulsion). Bubbles in fluidized beds are very important for they are responsible for most of the features which differentiate a fixed from a fluidized bed. They modify gas flow through the system and induce and influence particle movement and mixing which are responsible for high heat-transfer rates between the bed and immersed surfaces. The heat-transfer mechanism between gas fluidized beds and immersed surfaces has been long established. Bubbles act as stirring agents and thus

*Present address: Central Electricity Research Laboratories, Leatherhead, Surrey, England.

cause a continual mixing of the system. Regions of high heat capacity (packets of emulsion phase) are brought into contact with the heat transfer surface where they act as local heat sources or sinks and the heat is transferred by a non-steady heat-transfer process.

The simplest model of heat transfer based on the above mechanism was developed by Mickley and Fairbanks [1]. This model gives good qualitative agreement between theory and experiments but fails for short residence times of the packets of emulsion on the heat-transfer surface. It is shown in a recent paper [2] that the basic Mickley and Fairbanks model can be extended to describe heat transfer at surfaces in gas fluidized beds to a high degree of accuracy by introducing a property boundary layer in the vicinity of the heat-transfer surface. It is argued [2] that the property boundary layer is a result of voidage variation within the packets of emulsion when in the vicinity of a surface.

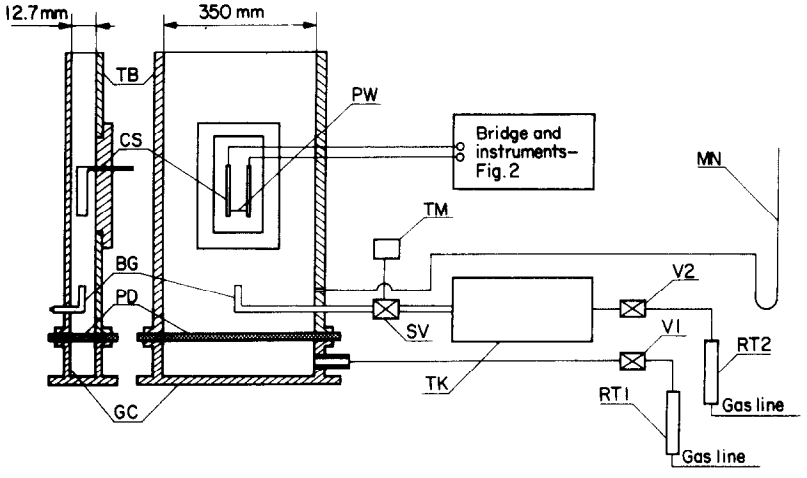

FIG. 1. Schematic diagram of the experimental apparatus.

It is shown in [2] that the thickness of the property boundary layer is of the order of one particle diameter. Hence for the property boundary layer to be controlling in determining heat-transfer rates, heat penetration depth from the surface to the packets of emulsion must be of the same magnitude. In order to satisfy this criterion experimentally, using a flat heat-transfer surface, either of the two following conditions must be fulfilled: (a) Instantaneous heat-transfer rates must be determined for short packet residence times on the surface, or (b) beds of large particles must be used. The former method introduces inaccuracies into the experimental technique, and the latter one is not reliable either, since additional heat-transfer mechanisms are introduced [3].

Because of the above mentioned difficulties, experimental evidence on the existence of the property boundary layer is inconclusive. It is one of the objects of this paper to submit further experimental justification for the method of defining and calculating the property boundary layer introduced in [2]. Further experimental evidence is obtained using a special heat-transfer probe [4–5] in beds of silica sands incipiently fluidized by widely different gases. It is demonstrated that if the property boundary layer is calculated by the method of [2], the theoretically obtained heat-transfer rates are in very good agreement with experimental data.

Further object of the reported work is to investigate the precise nature of the bubble induced heat-transfer mechanism in gas fluidized beds. Since it is difficult to investigate heat transfer in aggregative gas fluidized beds, the multibubbling system is simulated by generating a single continuous stream of gas bubbles into an incipiently fluidized bed. To compare various mechanisms of heat transfer and their contribution, a heat-transfer probe, which can be used to discriminate between conductive and convective modes of heat transfer [4 5], has been employed. A theoretical model of heat transfer, based on the surface renewal and penetration theory, has been developed and has been found to predict the bubble induced heat transfer to a good degree of accuracy.

2. EXPERIMENTAL

2.1. *Experimental apparatus*

The line diagram of the experimental equipment is shown in Fig. 1. To enable good observation of the bubble motion and to ensure uniform fluidization across the bed cross section, all experiments have been performed in a two-dimensional bed. The bed (TB), made of "perspex", 600 mm high, 350 mm wide and 12.7 mm thick, contains the solid particles. The bed is separated from the plenum chamber (GC) by a high pressure drop porous distributor (PD). The fluidizing gas is supplied through a valve (V1) and a rotameter (RT1), which measures the gas flow rate. The bubble generator (BG) is situated in the centre of the bed cross sectional area, about 30 mm above the distributor plate. The bubble generator consists of a thin stainless steel tube (1.6 mm in diameter) with a solenoid valve (SV)

at one end. The triggering signal for the solenoid valve is supplied by a triggering mechanism (TM) consisting of an electric motor, a series of cams and a microswitch. The gas to the bubble generator is supplied through a microrotameter (RT2) and a valve (V2). The tank (TK), placed between the valve (V2) and the solenoid valve (SV), is used to dampen pressure oscillations in the gas supply line, which are initiated by the action of the solenoid valve. The maximum frequency of bubble generation obtained with the present set up is about 2 bubbles per second. The heat-transfer probe, described below, is placed 80 mm above the generating orifice.

2.2. *The heat-transfer probe and its instrumentation*

The design of the probe is described in more detail elsewhere (Fig. 2 in [5]). A thin platinum wire (125 μm dia and 14.2 mm long), serving as the heat-transfer probe, is stretched between two flat copper supports. The wire is electrically heated and the copper supports serve as electric leads of negligible resistance. The probe construction is such that the length of the wire is equal (or about equal) to the diameter of the generated gas bubbles. The platinum wire has three basic functions [4–5]: (i) it serves as a heat-transfer probe; (ii) using the principles of anemometry it is employed to measure its own instantaneous temperature; (iii) it is used to measure the frequency of bubble generation.

This has been achieved by incorporating the probe into one branch of a standard Wheatstone bridge—Fig. 2. The current through the bridge is supplied by a 12 V battery (BT), the digital voltmeter (DV) is used to measure the voltage across the wire and the UV-recorder (UV) to record voltage fluctuations across the bridge.

2.3. *Experimental technique*

Experimental technique is described only briefly; more detailed description being given in [4–5].

Silica sand particles of various size ranges and five different gases were used for the experimental investigation. Their properties, at 25°C, are shown in Table 1. Solid particles were carefully graded on a sieving machine and very close size ranges were obtained. The mean particle diameter used is the geometric mean, calculated from the two sieve sizes which specify each size range. Mean emulsion voidage, ε_E, was determined experimentally from the volume of emulsion and the true density of the solid particles. The thermophysical properties of the emulsion were calculated by the method of [2, 6].

Table 1. Thermophysical properties of solid particles and gases at 25°C

	Size range	Mean diameter	k	c_P	ρ
	(μm)	(μm)	(W/mK)	(J/kgK)	(kg/m^3)
silica sand 1	75–90	82			
silica sand 2	125–180	150	1.87	860	2600
silica sand 3	250–300	274			
silica sand 4	500–600	548			
helium			0.148	5200	0.165
air			0.026	1008	1.19
argon			0.0177	520	1.63
carbon dioxide			0.016	850	1.79
freon 12			0.0097	650	5.14

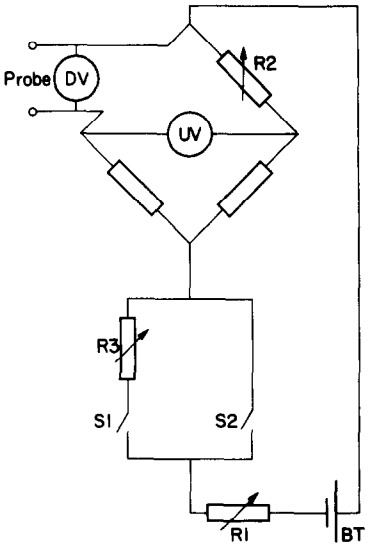

FIG. 2. Supporting bridge and instrumentation of the heat-transfer probe.

The condition of incipient fluidization was determined experimentally by a combination of pressure drop measurements through the bed and visual observations. It was difficult to generate gas bubbles into an incipiently fluidized bed, since the generated bubbles were unstable and each bubble was accompanied by a swarm of smaller bubbles which followed in its wake. It was found by a trial and error method that when the bed was fluidized at about 95% of incipiently fluidized conditions, stable bubbles could still be generated and maintained, but that the smaller bubbles following the main one were eliminated. (The 95% incipiently fluidized bed is for convenience referred to henceforth as the "incipiently fluidized bed".) The frequency of bubble generation was controlled by the speed of the cam and their volumes by the design of the cam and the gas back pressure in the tank. Volumes of generated bubbles were determined approximately

from the rate of the gas supply to the tank and the known frequency of bubble generation.

The wire was calibrated in water at known temperatures and the relationship between the wire temperature and the resistance of the variable resistor R2 (the calibration curve) was determined.

It is shown later (Section 3.6) that a possible way to investigate the property boundary layer is to apply a step heating input into the wire whose initial temperature is equal to the temperature of the surrounding emulsion. This is achieved by applying a very small current through the wire. This small current is used to balance the bridge, with the wire set at the temperature of the surrounding emulsion. (This is accomplished by connecting the switch S1 with a high resistance variable resistor R3 in its branch and by disconnecting the switch S2—Fig. 2.) Hence the switch S1 can be connected throughout the process, supplying the small current which is used to determine the initial temperature of the wire and of the emulsion, T_x. Then at certain time $t = 0$, switch S2 is connected too, thus supplying the full working heating load into the probe wire. The heating input generated within the wire can be approximated very well by a step function starting at time $t = 0$. The wire response is evaluated from the UV-recorder traces and calculated calibration constants [4].

To investigate the mechanism of the bubble induced heat transfer the procedure was as follows [4–5]: For a given frequency of bubble generation, the time-mean wire temperature was set approximately at the required level by setting the resistor R2 at a value corresponding to this temperature and by adjusting the current through the bridge (with the switch S2 connected) in such a way that the bridge was approximately in balance. Once the bridge was roughly balanced, the UV-recorder traces were obtained and used to calculate the variation of the instantaneous wire temperature with time. The exact time-mean average wire temperature was then calculated over the whole heating cycle [5] by graphical integration.

The frequency of bubble generation was then determined from the frequency of the periodic fluctuations of the instantaneous wire temperature. The rate of heat generation per unit volume of the wire, Q, was calculated from the voltage drop across the wire and the average wire resistance corresponding to the time-mean average wire temperature.

2.4. *Experimental results*

Experimental results are plotted in Figs. 5–15 and are discussed in Section 4. Except in Fig. 15, experimental results are presented in dimensionless form as graphs of Nusselt numbers vs corresponding Fourier numbers. The experimental instantaneous Nusselt number, $(Nu_X)_i$, corresponding to a particular value of the instantaneous Fourier number, Fo, is calculated from the known values of the rate of heat generation per unit volume of the wire, Q, and the instantaneous average temperature difference $\Delta T_i = (T_X)_i - T_\infty$. Similarly, the experimental time-mean Nusselt numbers are calculated as functions of the time-mean Fourier numbers.

The temperature of the bed for all experiments was set at 20°C and the time-mean average temperature difference, ΔT_m, was kept between 10 and 20°C.

3. THEORETICAL ANALYSIS

3.1. *Extended emulsion phase model of heat transfer*

The model is based on the work of Mickley and Fairbanks [1] who consider a packet of constant voidage emulsion being swept into contact with the heat-transfer surface for a period of time. They assume that during the packet residence on the heat-transfer surface, heat is transferred by a transient process.

In a recent paper [2], the emulsion phase model was extended. Assumptions of the extended theory, applicable to the present case, are summarized as follows:

(i) The emulsion phase has a constant voidage and is isothermal when in the bulk of the bed.

(ii) The only constraint on the position of particles in the packet of emulsion at the surface is provided by the surface itself, which influences the local packing and hence alters local thermophysical properties. Thus a concept of a property boundary layer is introduced. The extended theory will be used in the present paper.

3.2. *Assumptions used in the theoretical model*

A theoretical model of heat transfer, similar to that used in [5] has been developed. The model is based on the following assumptions:

(i) The heat-transfer process is periodic with period $\tau = 1/f$, where f is the frequency of bubble generation.

(ii) When a bubble passes the surface of the heat-transfer probe, the "old" emulsion, which has been heated by the wire prior to the bubble arrival, is replaced by "fresh" emulsion from the isothermal bulk of the bed, which was brought by the passing bubble in its wake. While this emulsion is in contact with the heat-transfer probe, heat is transferred by a non-steady heat-transfer process. After a certain time, the next bubble arrives and the whole process is repeated. In this way the emulsion on the surface of the probe is being replaced periodically at frequency $1/\tau$.

The next set of assumptions follows from the special construction of the present heat-transfer probe. It defines the model completely and may be summarized as follows:

(iii) The diameter of the passing bubbles is approximately equal to the length of the probe wire. Hence it is assumed that the emulsion is being effectively replaced over the whole surface area of the heat-transfer probe. It is further assumed that the residence time of gas bubbles on the surface of the heat-transfer probe is negligible compared with the residence time of the emulsion there. This implies that only emulsion is in contact with the surface of the heat-transfer probe.

(iv) Since the length of the probe wire is many times greater than the thickness of the property boundary layer and since, from the point of view of heat transfer, the copper supports provide only secondary heat-

transfer surfaces, it is assumed that the thickness of the property boundary layer of the emulsion in the vicinity of the copper supports is zero. Hence the concept of the property boundary layer will be applied on the probe wire only, resulting in the assumption that the thermophysical properties of the emulsion vary in the radial direction only. It is further assumed that all wire material properties and the emulsion properties outside the property boundary layer remain constant.
(v) It is further assumed that the radial extent of the copper supports and of the emulsion between them is infinite, compared with the very small radius of the probe wire. Hence the system may be regarded as axisymmetric about the x-axis.
(vi) Since the electrical and thermal resistances of the copper supports are small compared with those of the wire material and their surface area is large compared with that of the wire, it is assumed that they remain at the bed temperature, T_∞, throughout the process.
(vii) Since the wire is very thin and is made of material whose thermal conductivity is very much greater than that of its surrounding emulsion, the radial distribution of temperature within the wire will be nearly uniform. The wire then may be for many purposes regarded as a finite rod with heat generated within it and being dissipated (a) from the outer surface to the surrounding emulsion and (b) from its ends by conduction to the copper supports [7].
(viii) Finally it is assumed that the whole system operates below the radiative temperature level and that only the resistance heating of the wire is considered.

In order to make the mathematical description of the system simpler, the bed temperature is set at the reference zero ($T_\infty = 0$). Only the slab of the emulsion between the two copper supports is considered and it is assumed that each heating period starts at the moment when the emulsion on the wire surface has just been renewed. Using the above assumptions the full energy description of the process can be obtained. The energy equations together with momentum and continuity equations provide the complete description of the system. Thus, at least in principle, the solution could be obtained.

3.3. *Non-steady heat-transfer mechanism*

The system of differential equations describing the bubble induced heat transfer in the present system [4] is very complex and to solve would be extremely difficult. So an alternative method of solution, based on separating conductive and convective modes of heat transfer, has been developed [4–5].

While the wire is in contact with the surrounding emulsion, the heat is transferred from the wire to the emulsion by a non-steady heat-transfer process. Neglecting radiation, the remaining components of heat transfer can be defined as follows:
(i) Conduction into the stationary emulsion, called emulsion conduction.
(ii) Convection due to the moving emulsion, called emulsion convection. In the present system, emulsion convection is mainly due to the emulsion moving with the bubble wake.
(iii) Convection due to the superimposed gas flow through the interstices between the particles in the emulsion phase, called gas convection. The feature of gas fluidized beds is that gas is flowing upward through the bed of particles, providing an additional mechanism of surface-to-bed heat transfer. (The difference between emulsion and gas convection is that emulsion convection is defined here as due to the particles and gas moving simultaneously and gas convection as due to the contribution of gas moving faster than the emulsion.) Provided that the diameter of the solid particles is small, the gas velocity is generally small too and hence the contribution of gas convection can usually be neglected.

The convective components of the heat-transfer mechanism can be calculated only after the velocity fields in the wire vicinity have been determined. The calculation of the velocity fields in the wire vicinity causes the main difficulties in finding a full solution.

The method of solution employed here is in two parts: first, conductive heat transfer from the probe to the surrounding emulsion is calculated theoretically. Second, the effects of emulsion and gas convection are then determined by comparing the experimentally observed heat transfer from the probe under mixed mode conditions (emulsion conduction, emulsion convection and gas convection) with that one determined theoretically, in which emulsion conduction is the only mode of heat transfer. Thus in the subsequent theoretical analysis the effects of additional convections are neglected and it is assumed that emulsion conduction is the only mode of heat transfer. If the experimental heat-transfer rates are higher than the theoretical ones, which assume that emulsion conduction is the only mechanism of heat transfer, emulsion and gas convection provide important contributions to the heat transfer and their importance can be assessed from the difference between experimental and theoretical results.

3.4. *Influence of the initial wire temperature*

At the start of each heating cycle, when the emulsion has just been replaced on the surface of the probe wire, the initial temperature of the emulsion in the wire vicinity is the same as the temperature of the emulsion in the bulk of the bed, T_∞. Since the probe wire has finite heat capacity, finite times are required for finite changes of the wire temperature. Hence the initial wire temperature is different from the initial temperature of the emulsion. The initial wire temperature depends on many factors, such as the bubble residence time on the wire surface, thermophysical properties of the bubble gas etc. To discuss the influence of the initial wire temperature, T_0, the energy equations are presented in the following way:

Let

$$T_E = T_{E1} + T_{E2} \tag{1}$$

$$T_W = T_{W1} + T_{W2} \tag{2}$$

such that

$$t \geqslant 0, \quad r \geqslant a, \quad |x| \leqslant L$$

$$\rho(r)c_p(r)\frac{\partial T_{E1}}{\partial t} = k(r)\left(\frac{\partial^2 T_{E1}}{\partial r^2}+\frac{1}{r}\frac{\partial T_{E1}}{\partial r}+\frac{\partial^2 T_{E1}}{\partial x^2}\right)+\frac{\mathrm{d}k(r)}{\mathrm{d}r}\frac{\partial T_{E1}}{\partial r} \quad (3)$$

$$t \geqslant 0, \quad r \leqslant a, \quad |x| \leqslant L$$

$$(\rho c_p)_W \frac{\partial T_{W1}}{\partial t} = k_W\left(\frac{\partial^2 T_{W1}}{\partial r^2}+\frac{1}{r}\frac{\partial T_{W1}}{\partial r}+\frac{\partial^2 T_{W1}}{\partial x^2}\right)+Q \quad (4)$$

subject to

$$t = 0,\ r > a,\ |x| \leqslant L \qquad T_{E1} = 0 \quad (5)$$

$$t = 0,\ r \leqslant a,\ |x| \leqslant L \qquad T_{W1} = 0 \quad (6)$$

$$t \geqslant 0,\ r > a,\ |x| = L \qquad T_{E1} = 0 \quad (7)$$

$$t \geqslant 0,\ r \leqslant a,\ |x| = L \qquad T_{W1} = 0 \quad (8)$$

$$t \geqslant 0,\ r > a,\ x = 0 \qquad \partial T_{E1}/\partial x = 0 \quad (9)$$

$$t \geqslant 0,\ r \leqslant a,\ x = 0 \qquad \partial T_{W1}/\partial x = 0 \quad (10)$$

$$t \geqslant 0,\ r = a,\ |x| \leqslant L \qquad T_{E1} = T_{W1} \quad (11)$$

$$t \geqslant 0,\ r = a,\ |x| \leqslant L \qquad -k(a)\frac{\partial T_{E1}}{\partial r} = -k_W\frac{\partial T_{W1}}{\partial r} \quad (12)$$

and

$$t \geqslant 0, \quad r \geqslant a, \quad |x| \leqslant L$$

$$\rho(r)c_p(r)\frac{\partial T_{E2}}{\partial t} = k(r)\left(\frac{\partial^2 T_{E2}}{\partial r^2}+\frac{1}{r}\frac{\partial T_{E2}}{\partial r}+\frac{\partial^2 T_{E2}}{\partial x^2}\right)+\frac{\mathrm{d}k(r)}{\mathrm{d}r}\frac{\partial T_{E2}}{\partial r} \quad (13)$$

$$t \geqslant 0, \quad r \leqslant a, \quad |x| \leqslant L$$

$$(\rho c_p)_W \frac{\partial T_{W2}}{\partial t} = k_W\left(\frac{\partial^2 T_{W2}}{\partial r^2}+\frac{1}{r}\frac{\partial T_{W2}}{\partial r}+\frac{\partial^2 T_{W2}}{\partial x^2}\right) \quad (14)$$

subject to

$$t = 0,\ r > a,\ |x| \leqslant L \qquad T_{E2} = 0 \quad (15)$$

$$t = 0,\ r \leqslant a,\ |x| \leqslant L \qquad T_{W2} = T_0(r, x) \quad (16)$$

$$t \geqslant 0,\ r > a,\ |x| = L \qquad T_{E2} = 0 \quad (17)$$

$$t \geqslant 0,\ r \leqslant a,\ |x| = L \qquad T_{W2} = 0 \quad (18)$$

$$t \geqslant 0,\ r > a,\ x = 0 \qquad \partial T_{E2}/\partial x = 0 \quad (19)$$

$$t \geqslant 0,\ r \leqslant a,\ x = 0 \qquad \partial T_{W2}/\partial x = 0 \quad (20)$$

$$t \geqslant 0,\ r = a,\ |x| \leqslant L \qquad T_{E2} = T_{W2} \quad (21)$$

$$t \geqslant 0,\ r = a,\ |x| \leqslant L \qquad -k(a)\frac{\partial T_{E2}}{\partial r} = -k_W\frac{\partial T_{W2}}{\partial r}. \quad (22)$$

The solution of equations (13)–(22) provides only a transient non-trivial temperature field, due to the influence of the non-zero initial wire temperature. The importance of this solution can be summarized by the following statement [5]: The greater the instantaneous Fourier number, Fo, the smaller the influence of the non-zero initial wire temperature on the total temperature field in and around the wire. Hence the solution of equations (3)–(12) will provide the first approximation to the temperature field in and around the wire when emulsion conduction is the only mechanism of heat transfer, and its accuracy will increase with increasing values of the instantaneous Fourier number.

The solutions of above equations will provide the local wire temperature. In order to compare theoretical and experimental results with as low error as possible, it is desirable to express the theoretical solution in terms of directly measurable variables. It is shown in [5] that one of these directly measurable parameters is the space-average wire temperature, T, (hereafter referred to as "average wire temperature") defined as

$$T = \frac{1}{2L}\int_{-L}^{L} T_W \,\mathrm{d}x \quad (23)$$

where T_W is the local wire temperature distribution.

Thus the instantaneous average wire temperature, T_i, at any time t may be obtained. From the point of view of overall time-mean heat transfer, the time-mean average wire temperature, T_m, is of far greater importance. In the present case, the time-mean average wire temperature, T_m, is defined as [5]

$$T_m = \frac{1}{\tau}\int_0^{\tau} T_i \,\mathrm{d}t \quad (24)$$

where τ is the periodic time of bubble generation.

In order to proceed with numerical calculations, the variation of the thermophysical properties with the radial distance in the property boundary layer must be determined. This is done in the next Section.

3.5. *Property boundary layer*

Once the voidage variation in the vicinity of the probe wire is determined, the variation of the thermophysical properties within the property boundary layer can be calculated too.

The method of calculating the voidage variation in the vicinity of the probe wire is analogous to that discussed in [2]. Since the wire radius is comparable with the radius of the solid particles in the emulsion, the curvature of the probe wire must be taken into account when calculating the voidage distribution in the wire vicinity. As mentioned in [2], particles at the same distance from the constraining wall (probe wire in the present case) are influenced by it in the same way. Hence the mean voidage at any cylindrical plane, concentric with the probe wire, is a function of the distance of this cylindrical plane from the probe wire.

It is shown in Appendix 1 that to calculate the voidage distribution in the wire vicinity, the solid concentration there must be known. Hence analogously to [2], it is postulated: For a bed of uniform spherical particles, the solid cross sectional area on a particular cylindrical reference plane, distance Δr from the probe wire, is proportional to the cross sectional area of a cylinder whose volume and height are identical to those of that part of the spherical particle which can be found in the annulus of the reference cylinder and the probe wire, while touching the probe wire— Fig. A1. The method of calculation of the voidage distribution, $\varepsilon(r)$, in the wire vicinity is described in detail in Appendix 1. The predicted distributions of the voidage, $\varepsilon(r)$, in the wire vicinity for three ratios of the wire and the particles radii are plotted in Fig. 3.

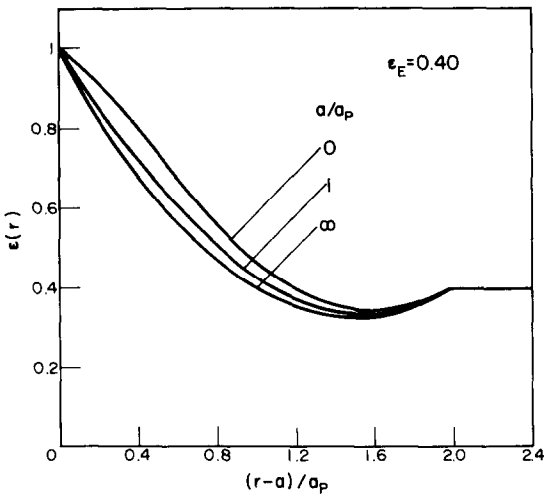

FIG. 3. Variation of the emulsion phase voidage in the wire vicinity.

From the calculated values of the voidage in the wire vicinity, the variations of the thermophysical properties within the boundary layer can be obtained [4–5] as

$$\rho(r)c_p(r) = (\rho c_p)_P[1-\varepsilon(r)] \tag{25}$$

and

$$k(r) = fn[k_P, k_G, \varepsilon(r)]. \tag{26}$$

Figure 4 shows the behaviour of thermal conductivity of the emulsion, $k(r)$, in the wire vicinity for three ratios of the wire and the particles radii and two particular values of the gas and the particles thermal conductivities.

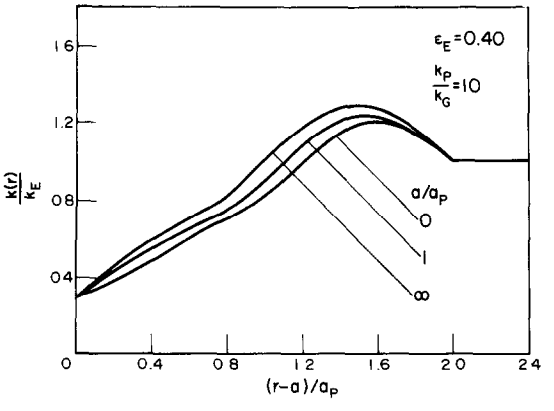

FIG. 4. Variation of the emulsion phase conductivity in the wire vicinity.

3.6. *First approximation and its application*

It can be shown that were conduction the only mechanism of heat transfer between the probe and the surrounding emulsion, the first approximation to the temperature field in and around the wire [equations (3)–(12)] would be equivalent to the exact solution of an identical system where a step heating input is applied to the wire whose initial temperature is the same as the initial temperature of the surrounding emulsion ($T_\infty = 0$).

If the wire is placed in a stationary emulsion of small particles, there are no convection currents within the emulsion and gas convection contribution to the overall heat transfer is small. Hence after applying a step heating input into the wire, which is placed in a stationary emulsion of small particles, conduction into the emulsion is the only mechanism of heat transfer between the wire and the surrounding emulsion. (The stationary emulsion is obtained by suppressing the generation of gas bubbles and the step heating input is generated by the method of Section 2.3.)

The only parameters in equations (3)–(12) which are not well defined are the thermophysical properties of the emulsion within the boundary layer. Hence the agreement (or otherwise) between the theoretical description, given by equations (3)–(12), with the thermophysical properties calculated by the method of Section 3.5, and the experimental results obtained by applying a step heating input into the wire in a stationary emulsion of small particles can be used as a criterion in regarding the merits (or otherwise) of the assumptions used in defining the property boundary layer. This technique can be used to obtain further experimental evidence for justifying the concept of the property boundary layer developed in [4–5].

Equations (3)–(12) can be solved numerically if all parameters of a particular system are known. The method of the numerical solution is briefly discussed in Appendix 2. Hence, finally, the first approximations to the instantaneous and the time-mean average wire temperatures [$(T_1)_i$ and $(T_1)_m$ respectively] can be obtained. Theoretical predictions are compared with the experimental data in Figs. 5–8.

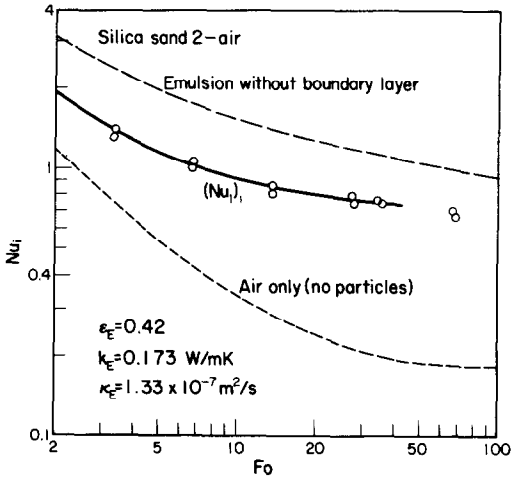

FIG. 5. Response of the wire, placed in an incipiently fluidized bed of silica sand 2–air, to a step heating input (○ —experimental points).

3.7. *Conduction model of the bubble induced heat transfer*

The temperature field due to the influence of the initial wire temperature is given by the solution of equations (13)–(22). The solution is obtained numerically by a method identical to that of [5]. Hence the instantaneous, $(T_2)_i$, and the time-mean, $(T_2)_m$, average wire temperatures due to the initial wire temperature, T_0, can be calculated.

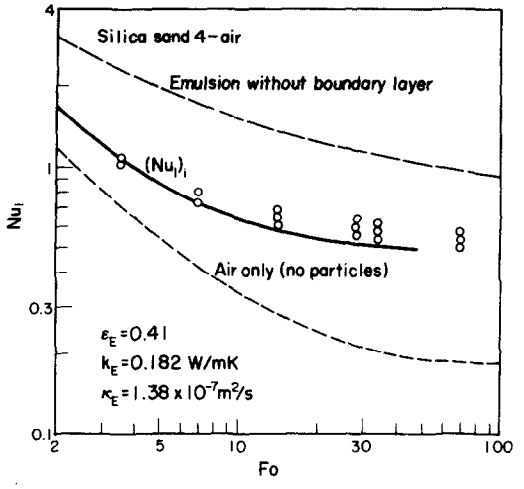

FIG. 6. Response of the wire, placed in an incipiently fluidized bed of silica sand 4–air, to a step heating input (○—experimental points).

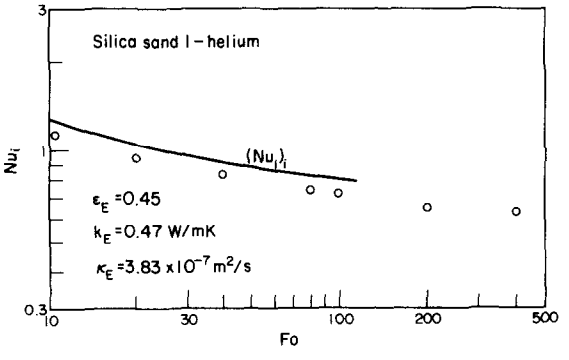

FIG. 7. Response of the wire, placed in an incipiently fluidized bed of silica sand 1–helium, to a step heating input (○—experimental points).

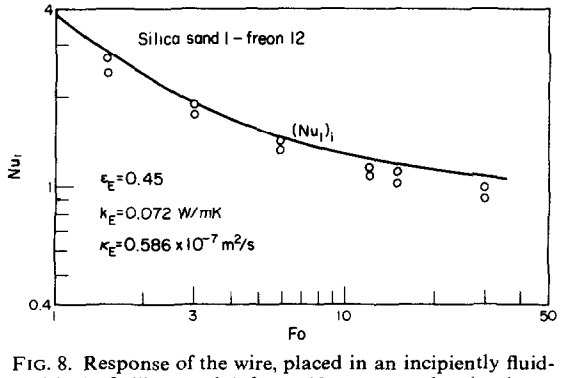

FIG. 8. Response of the wire, placed in an incipiently fluidized bed of silica sand 1–freon 12, to a step heating input (○—experimental points).

Full solution for the temperature field in and around the wire is defined by equations (1)–(2). Similarly the instantaneous and the time-mean average wire temperatures can be defined, in dimensionless form, as [5]

$$\frac{T_i k_E}{Qa^2} = \frac{(T_1)_i k_E}{Qa^2} + \frac{(T_2)_i}{T_{0A}} \frac{[(T_X)_m - T_\infty]k_E}{Qa^2} \tag{27}$$

$$\frac{T_m k_E}{Qa^2} = \frac{(T_1)_m k_E}{Qa^2} + \frac{(T_2)_m}{T_{0A}} \frac{[(T_X)_m - T_\infty]k_E}{Qa^2} \tag{28}$$

where T_{0A}, the initial average wire temperature, is given approximately [4–5] as

$$T_{0A} = (T_X)_m - T_\infty. \tag{29}$$

It can be shown [5] that $Qa^2/(T_1)_i k_E$ and $Qa^2/(T_1)_m k_E$ can be regarded as first approximations to the instantaneous and the time-mean Nusselt numbers respectively. Furthermore, for the above value of the initial average wire temperature, $T_{0A} = (T_X)_m - T_\infty$, the group $Qa^2/[(T_X)_m - T_\infty]k_E$ is equal to the experimentally determined time-mean Nusselt number, $(Nu_X)_m$.

Hence

$$(Nu_1)_i = \frac{Qa^2}{(T_1)_i k_E} \tag{30}$$

$$(Nu_1)_m = \frac{Qa^2}{(T_1)_m k_E} \tag{31}$$

where $(Nu_1)_i$ and $(Nu_1)_m$ are first approximations to the instantaneous and the time-mean Nusselt numbers respectively.

Similarly

$$Nu_i = 1\Big/\left[\frac{1}{(Nu_1)_i} + \frac{(T_2)_i}{T_{0A}} \frac{1}{(Nu_X)_m}\right] \tag{32}$$

$$Nu_m = 1\Big/\left[\frac{1}{(Nu_1)_m} + \frac{(T_2)_m}{T_{0A}} \frac{1}{(Nu_X)_m}\right] \tag{33}$$

where Nu_i and Nu_m are full solutions for the instantaneous and the time-mean Nusselt numbers respectively.

The theoretical predictions are compared with the experimental data in Figs. 9–13.

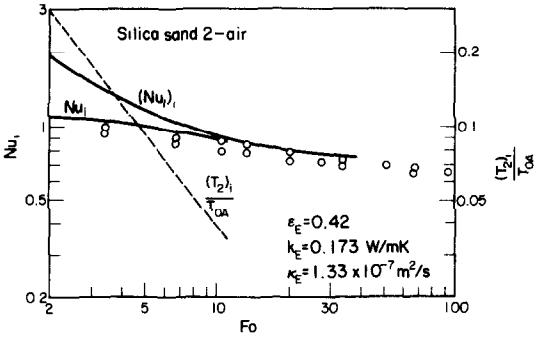

FIG. 9. Instantaneous bubble induced heat transfer from the wire to an incipiently fluidized bed of silica sand 2–air (○—experimental points).

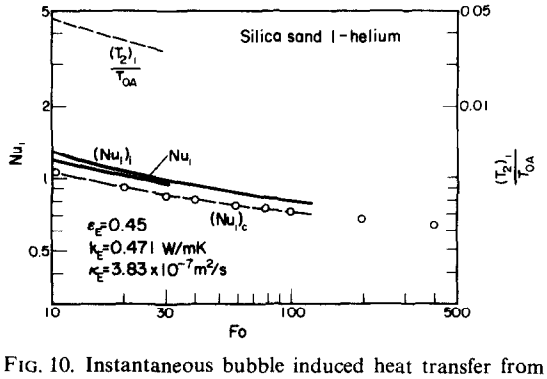

FIG. 10. Instantaneous bubble induced heat transfer from the wire to an incipiently fluidized bed of silica sand 1–helium (○—experimental points).

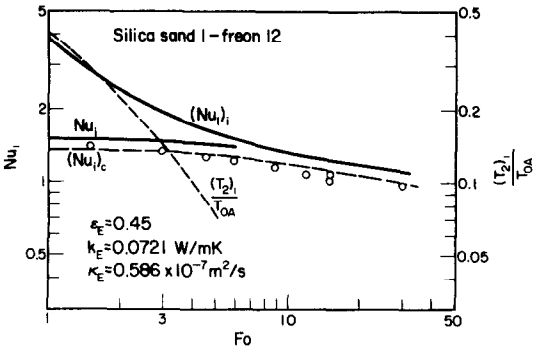

FIG. 11. Instantaneous bubble induced heat transfer from the wire to an incipiently fluidized bed of silica sand 1–freon 12 (○ —experimental points).

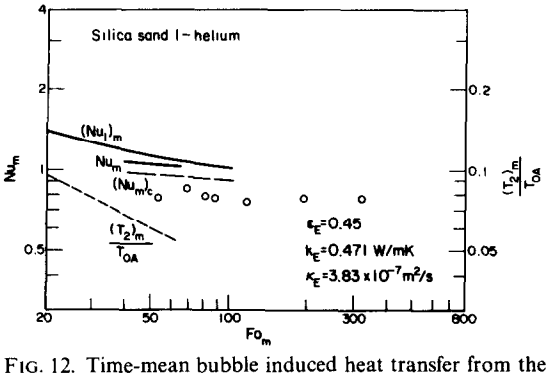

FIG. 12. Time-mean bubble induced heat transfer from the wire to an incipiently fluidized bed of silica sand 1–helium (○ —experimental points).

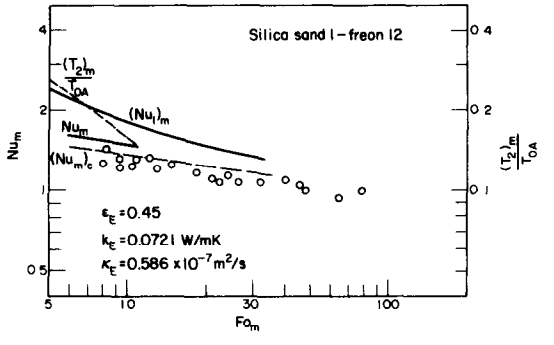

FIG. 13. Time-mean bubble induced heat transfer from the wire to an incipiently fluidized bed of silica sand 1–freon 12 (○ —experimental points).

4. DISCUSSION

4.1. *Influence of gas convection*

It has been shown in Section 3.6 that when the heat-transfer probe is placed in a stationary (or a fixed) bed and a step heating input is applied into the probe wire, the only mechanisms of heat transfer between the probe and the surrounding emulsion are gas convection and emulsion conduction. In this work, the contribution of gas convection was determined as follows: The probe was placed into a fixed bed and a step heating input was applied into the wire. The gas flowrate was then increased in steps to 95% of incipient fluidization and the step heating input into the wire was applied for each value of the gas flowrate. The contribution of gas convection was then obtained from the difference in heat transfer rates (responses of the wire) between cases of zero gas velocity and the gas velocity at 95% of incipient fluidization.

Because in incipiently fluidized systems gas velocities increase with the particle size [8], the contribution of gas convection is greater in gas fluidized beds of coarse particles.

Figure 14 shows that for the largest particles used in the present investigation (silica sand 4), with air as the gas phase, the contribution of gas convection to the total heat transfer is about 10%. Experiments were also conducted to determine the contribution of gas convection in beds of silica sand 1, 2 and 3. There the contribution of gas convection is so small that it cannot be determined by the present experimental technique.

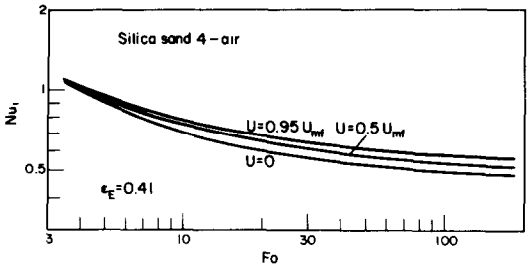

FIG. 14. Influence of gas velocity on the response of the wire, placed in a bed of silica sand 4–air, to a step heating input (○ —experimental points).

Hence by using silica sand of size ranges below 600 μm, the contribution of gas convection can be kept small, and by using silica sand of size ranges below 300 μm, the contribution of gas convection can be neglected. This agrees well with experimental data of other investigators [9–10].

4.2. *Concept of the property boundary layer*

The situation where the heat transfer probe is placed in an incipiently fluidized bed of small particles was discussed in Section 3.6, where it was shown that under those circumstances the only mechanism of heat transfer following a step heating input into the wire is emulsion conduction.

Figures 5–8 demonstrate very good agreement between experimental data and theoretical predictions. With exception of silica sand 4/air (Fig. 6), experimental data fall below the corresponding theoretical predictions. With increased particle size the experimental points get nearer to, or even above (Fig. 6), the theoretical curve. This is due to the contribution of gas convection which increases with increasing particle size (Section 4.1) and hence causes an increase in experimental heat-transfer rates, which is most prominent in the case of silica sand 4/air (Fig. 6). Hence one can assume that were the effect of gas convection taken into account and subtracted, all experimental results would then fall below the theoretical predictions.

Hence assuming that conduction is the only mechanism of heat transfer between the wire and the surrounding emulsion, the theoretical results are higher than the experimental data by, on average [4], about 11%.

Since the numerical technique used here is sufficiently accurate [4], the above results indicate that some systematic error is being made during the theoretical calculation of the distribution of the thermophysical properties within the property boundary layer. But considering the wide range of particle sizes used (75–600 μm) and the wide range of the gas thermal conductivities (0.0097–0.148 W/mK), the agreement may be regarded as satisfactory. It is doubtful if any refinement of the method of calculating the thermophysical properties is required, since the present method gives good agreement with experimental data and is based on simple geometrical considerations and well established techniques [2, 6].

Figures 5–6 demonstrate the importance of the concept of the property boundary layer. Both figures contain also two theoretical solutions based on the respective assumptions that (a) the emulsion phase behaves as a uniform medium with constant thermophysical properties everywhere, even in the vicinity of the probe wire, and (b) that only the stationary gas (and not the solid particles), is present in the system. The theoretical solutions have been obtained from [5] – equation (28), using the thermophysical properties of the emulsion and of the fluidizing gas respectively. One can observe that if the property boundary layer is not considered the theoretical predictions diverge greatly from the experimental results. Since the property boundary layer is one particle diameter thick, the concept of the property boundary layer is more important for fluidized beds of coarser particles (Figs. 5 and 6).

The excellent agreement between the theoretical and experimental results provides a powerful argument for the justification of the concept of the property boundary layer and hence for the model of heat transfer in gas fluidized beds, developed in [2].

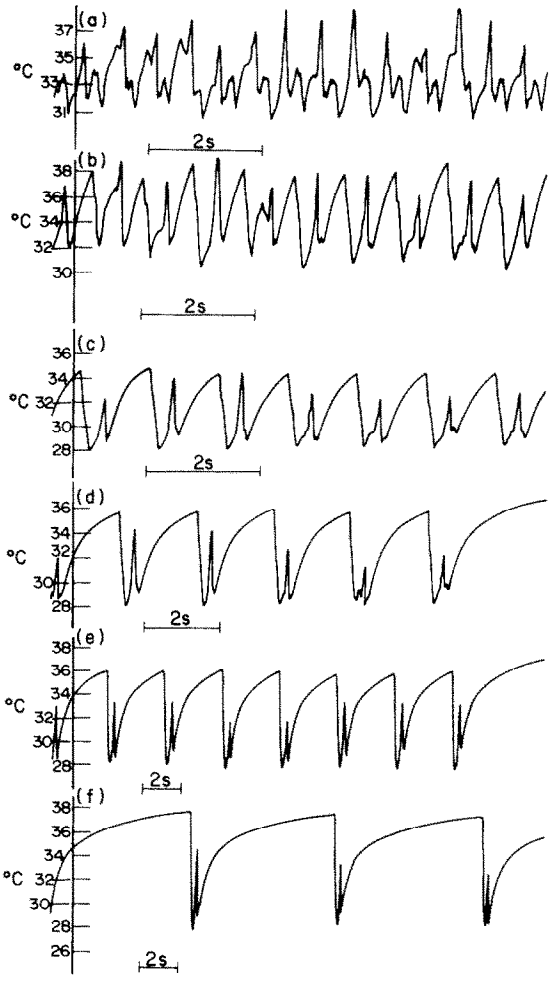

FIG. 15. Variation of the instantaneous average wire temperature with time (incipiently fluidized bed of copper shot–air). From top to bottom: f = 1.7, 1.1, 0.83, 0.49, 0.33, 0.13 l/s.

4.3. *Instantaneous average wire temperature*

The variation of the instantaneous average wire temperature with time for various frequencies of bubble generation is shown in Fig. 15. This figure was obtained by photographing some of the UV-recorder traces. These temperature variations have been obtained by placing the probe into an incipiently fluidized bed of copper shot (a_P = 130 μm). Copper shots were chosen because the shape of generated bubbles was well defined and reproducible, and, further because it was relatively simple to keep the bed at incipiently fluidized conditions. Similar, but not so well defined graphs, were obtained also for fluidized beds of silica sand. The explanation of the temperature–time profiles of Fig. 15 is identical to that suggested in [5].

4.4. *Bubble induced heat transfer*

It is shown in [4] that the numerical technique used here is sufficiently accurate. Hence the theoretically derived solutions for the instantaneous bubble induced heat transfer from the wire to the surrounding emulsion, based on transient conduction as the only mechanism of heat transfer, should result in heat-transfer coefficients which are lower than those obtained experimentally. This must be the case because the additional mechanisms of heat-transfer (gas convection and emulsion convection), which increase the experimentally obtained heat-transfer coefficients, are neglected in the theoretical analysis. Because of the emulsion moving with the bubble wake, the effect of emulsion convection should be most prominent for short emulsion residence times and hence for small values of the instantaneous Fourier number, Fo. To decrease the influence of gas convection, particles of small diameters only have been used for the experimental investigation of the bubble induced heat transfer.

Experimental results of the instantaneous bubble induced heat transfer (obtained as discrete points by the method of [5]) are shown in Figs. 9–11.

Figures 9–11 demonstrate that, as in the case of the wire response to a step heating input (Section 4.2), the theoretical results are higher, on average by about 10%, than the experimental data. Assuming, as in Section 4.2, that the reason for this discrepancy is some systematic error, made during the calculation of thermophysical properties within the boundary layer, a correction can readily be made to take this effect into account. The theoretical heat-transfer coefficients for

the instantaneous bubble induced heat transfer are decreased by an amount which is equal to the difference between the theoretical and experimental results of heat transfer following a step heating input into the wire when submerged into an identical emulsion. This difference (or correction factor) for Figs. 9–11 is obtained from Figs. 5, 7, and 8 respectively. The corrected theoretical results are also included in Figs. 9–11.

The corrected theoretical results and the experimental data for the instantaneous bubble induced heat transfer are, within the range of experimental errors, nearly identical. This is consistent with the assumption that transient conduction is the most important mechanism of the bubble induced heat transfer in gas fluidized beds of small particles. The present experimental results indicate that transient conduction is responsible for nearly 100% of the total heat transfer and that the contribution of emulsion convection is almost negligible.

Some of the experimentally obtained time-mean bubble induced heat-transfer coefficients (in dimensionless form) are shown in Figs. 12–13. The theoretical results are also included and, using the method described above, they are again corrected to take into account the systematic error made during the theoretical calculations of the thermophysical properties. Even after taking into account this correction, theoretical predictions are in the regions where the theoretical solutions have been obtained slightly higher (on average about 10%) than the experimental data. This is probably due to the finite residence times of gas bubbles on the surface of the wire, τ_b.

The theoretical solutions are based on the assumptions that the residence time of gas bubbles on the surface of the wire is zero and that only the bubble wakes (and not the bubble "noses") are responsible for the renewal of the emulsion on the wire surface. Since the heat capacity of the gas is much smaller than the heat capacity of the emulsion, heat transfer from the wire to the surrounding gas during the bubble presence on the wire is very small and can be neglected.

If the bubble wakes only were responsible for the mechanism of surface renewal, the experimental results would be considerably smaller than the theoretical ones, calculated on the assumption that the residence time of gas bubbles on the wire surface is zero. It has been found during the present experimental work that the difference between the experimental and corrected theoretical results (and hence the influence of the finite bubble residence time on the wire surface) is not that profound. This then indicates that there must be an additional mechanism influencing the time-mean bubble induced heat transfer. This is the effect of the bubble "noses", which provide an additional mechanism of surface renewal of the emulsion on the wire surface, thus increasing the time-mean heat transfer and hence opposing the effect of the decreased heat-transfer rates during the residence of gas bubbles on the wire surface. The two effects cancel, at least partially, each other out. This can be seen in Fig. 15, where for the case of high frequencies of bubble generation the mutual elimination of both effects is best demonstrated.

It has been demonstrated that the frequency of bubble generation has a very strong influence on the time-mean bubble induced heat transfer. In order to maximize it, the frequency of bubble generation should be as high as possible, but care should be taken to ensure that the decrease of the time-mean heat transfer due to the bubble residence on the wire surface does not outweigh the favourable effects of high frequencies of bubble generation.

5. CONCLUSIONS

Bubble induced heat transfer in simplified gas fluidized systems, using a special heat-transfer probe, has been investigated. It has been found that:

(i) The method of defining and evaluating the property boundary layer, developed in [2, 4], gives very good agreement with experimental data. The use of the method results in theoretical heat-transfer coefficients which are, on average, about 10% above the comparable experimental data.

(ii) Surface renewal and penetration theory, developed here, with the property boundary layer calculated by the present method, can be used to describe the bubble induced heat transfer in the present system to a good degree of accuracy.

(iii) The bubble wakes are primarily responsible for the renewal of the emulsion on the wire surface, while their "noses" are shown to be responsible for at least some surface renewal of the emulsion. It has been shown that this action of the bubble "noses" increases the time-mean bubble induced heat transfer, cancelling, at least partially, the decrease of the heat transfer during the residence of gas bubbles on the surface of the wire. The theoretical time-mean heat-transfer coefficients can then be calculated on the assumption that the bubble wakes only are responsible for the surface renewal of the emulsion and the effect of the bubble "noses" and bubble residence times can be neglected. The theoretical results so obtained are in acceptable agreement with the experimental data obtained here.

(iv) Transient conduction into the emulsion is the most important mechanism of the bubble induced heat transfer, being responsible—in the present case—for more than 90% of the total heat transfer. The remainder is provided by superimposed gas convection, whose contribution increases with the mean particle size. The contribution of emulsion convection is shown to be very small and can be neglected.

(v) To maximize the time-mean bubble induced heat transfer the frequency of bubble generation should be as high as possible, but their volumes should be small so as to keep their residence time on the surface of the wire also small compared with the residence time of the emulsion there.

Acknowledgements—The author's thanks are due to The University of Aston in Birmingham for supporting this work. Thanks are also due to Professor D. E. Elliott of the Department of Mechanical Engineering, University of Aston, for his help and suggestions during the course of this work.

REFERENCES

1. H. S. Mickley and D. F. Fairbanks, Mechanism of heat transfer to fluidized beds, *A.I.Ch.E. Jl* **1**, 374 (1955).
2. J. Kubie and J. Broughton, A model of heat transfer in gas fluidized beds, *Int. J. Heat Mass Transfer* **18**, 289 (1975).
3. J. S. M. Botterill and M. Desai, Limiting factors in gas fluidized bed heat transfer, *Powder Technol.* **6**, 231 (1972).
4. J. Kubie, Bubble induced heat transfer in two-phase systems, Ph.D. Thesis, Dept. Mech. Engng, University of Aston in Birmingham, May (1974).
5. J. Kubie, Bubble induced heat transfer in two phase gas-liquid flow, *Int. J. Heat Mass Transfer* **18**, 537 (1975).
6. D. Kunii and J. M. Smith, Heat transfer characteristics of porous rocks, *A.I.Ch.E. Jl* **6**, 71 (1960).
7. J. C. Jaeger, Conduction of heat in a solid in contact with a thin layer of a good conductor, *Q. Jl Mech. Appl. Math.* **8**, 101 (1955).
8. J. F. Davidson and D. Harrison, *Fluidization*. Academic Press, London (1971).
9. A. P. Baskakov and V. M. Suprun, The determination of the convective component of the coefficient of heat transfer to a gas in a fluidized bed, *Int. Chem. Engng* **12**(1), 53 (1972).
10. T. Shirai, H. Yashitome, Y. Shaji, S. Tanaka, K. Hojo and S. Yoshida, Heat and mass transfer on the surface of solid spheres fixed with fluidized beds, *Kagaku Kogaku* (*Chem. Engng Japan*) **29**, 880 (1965).
11. K. Rektorys, *Survey of Applicable Mathematics*. Iliffe, London (1969).
12. H. S. Carslaw and J. C. Jaeger, *Conduction of Heat in Solids*, 2nd edn. Oxford University Press, Oxford (1959).

APPENDIX 1

Following [2] the solid concentration, $\beta(r)$, is given as

$$\Delta r \leqslant 2a_P \qquad \beta(r) = (1-\varepsilon_E)\frac{2a_P}{\Delta r}\frac{V(r)}{V_P} \tag{A1}$$

$$\Delta r > 2a_P \qquad \beta(r) = 1-\varepsilon_E \tag{A2}$$

where

$$\beta(r) = 1-\varepsilon(r) \tag{A3}$$

and where $\varepsilon(r)$ is the area voidage and $V(r)$, the volume of that part of a spherical particle which can be found in the annulus of the reference and the constraining cylinder (Section 3.5), is calculated as follows (Fig. A1):

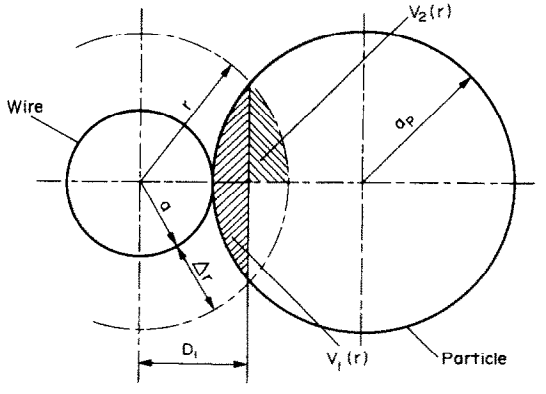

FIG. A1. A spherical particle in the wire vicinity.

Let

$$V(r) = V_1(r) + 4V_2(r) \tag{A4}$$

where $V_1(r)$ is the volume of that segment of the particle which is cut be a plane, distance D_1 from the origin, and $V_2(r)$ is the volume of a quarter of the remaining part of $V(r)$.

$V_1(r)$ is given by standard textbooks [11] as

$$V_1(r) = 0.5\pi(r^2-D_1^2)(D_1-a)+\tfrac{1}{6}\pi(D_1-a)^3 \tag{A5}$$

and $V_2(r)$ is calculated as follows

$$V_2(r) = \int_{D_1}^{r}\int_0^{\theta}\int_0^{z} r\,dz\,d\theta\,dr \tag{A6}$$

where

$$z = [a_P^2-(r-a-a_P)^2]^{1/2} \tag{A7}$$

$$\theta = \arctan[(r/D_1)^2-1]^{1/2}. \tag{A8}$$

Finally, after some rearranging and integrating we obtain [4]

$$R \leqslant 1+\frac{2}{\sigma}$$

$$\varepsilon(r) = 1-\frac{3(1-\varepsilon_E)}{2\pi\sigma(R-1)}\left\{\frac{\pi}{2}(\sigma^2R^2-\delta^2)(\delta-\sigma)+\frac{\pi}{6}(\delta-\sigma)^3 + 4\int_{\delta}^{\sigma R}\eta\,[1-(\eta-\sigma-1)^2]^{1/2}\arctan[(\eta/\delta)^2-1]^{1/2}\,d\eta\right\} \tag{A9}$$

$$R > 1+\frac{2}{\sigma}$$

$$\varepsilon(r) = \varepsilon_E \tag{A10}$$

where

$$R = r/a \tag{A11}$$

$$\sigma = a/a_P \tag{A12}$$

$$\delta = \frac{\sigma^2(R+1)+2\sigma}{2(\sigma+1)}. \tag{A13}$$

The numerical values of the voidage are then obtained by the numerical integration of (A9).

APPENDIX 2

The numerical technique is discussed more fully in [4]. First, all derivatives were rewritten using a standard difference technique [12]. In order to solve the difference equations accurately, very small space (and hence time) increments must be used, because the thermophysical properties vary very rapidly in the wire vicinity. In order to overcome this complication and thus decrease the computer time requirements, a concept of the equivalent thermal conductivity (analogous to that used in [2]) has been employed [4].

For each time interval the temperature field was calculated up to a point, distance Δr from the wire surface, where the temperature of the emulsion reached a prescribed small value. At this point the calculation was terminated and restarted for the next time interval. It was found that the accuracy of the numerical solution was relatively insensitive to the size of r-increments and $\Delta r = 0.2a$ to $0.25a$ could be used to achieve sufficient accuracy. On the other hand, the accuracy of the solution was very sensitive to the size of x-increments, but too small a value of the Δx-step size required very large computer times. Hence a compromise was reached by using Δx size of $0.25L$ to $0.33L$. The maximum error then was about 3% (as confirmed by decreasing the step size to obtain a check). The first approximation to the bubble induced heat transfer was calculated for emulsion residence times of up to 1 s. Since the calculation of the full solution of the bubble induced heat transfer required even longer times, the full solution was obtained for emulsion residence times of up to 0.3 s. This was regarded as a good compromise, since for larger emulsion residence times the first approximation to the bubble induced heat transfer becomes nearly identical with the full solution of the problem.

TRANSFERT DE CHALEUR INDUIT PAR LES BULLES DANS LES LITS FLUIDISES GAZEUX

Résumé—On présente une étude de l'influence des bulles de gaz sur le transfert de chaleur dans les lits fluidisés gazeux. Une sonde thermique constituée par un fil de platine a été utilisée et le lit préfluidisé a été schématisé en envoyant un courant continu de bulles gazeuses dans une couche. On montre que dans un lit préfluidisé gazeux de petites particules utilisé à un température inférieure au niveau de rayonnement, la conduction transitoire dans la phase émulsionnée est responsable d'au moins 90 pour cent du transfert thermique, le reste étant dû à la convection gazeuse surimposée. Un modèle théorique du transfert de chaleur induit par les bulles a été développé. On présente enfin une justification expérimentale du concept de couche limite d'une propriété quelconque, introduit dans [2].

DER EINFLUSS VON GASBLASEN AUF DEN WÄRMEÜBERGANG IN GASDURCHSTRÖMTEN WIRBELSCHICHTEN

Zusammenfassung—Es wurde der Einfluß von Gasblasen auf den Wärmeübergang in gasdurchströmten Wirbelschichten untersucht. Als Wärmeübergangs- Meßsonde wurde ein Platin-Draht verwendet; die brodelnde Wirbelschicht wurde vereinfacht dargestellt durch einen einzigen, kontinuierlichen Gasblasenstrom in eine frisch aufgewirbelte Schicht. Für brodelnde, mit kleinen Partikeln beschickte Wirbelschichten, welche unterhalb der Strahlungstemperaturgrenze betrieben werden, ergab sich, daß instationäre Wärmeleitung in die Emulsionsphase für wenigstens 90% des Wärmeübergangs verantwortlich ist; die restlichen 10% werden der überlagerten Gaskonvektion zugeschrieben. Es wurde ein theoretisches Modell für den durch die Blasen hervorgerufenen Wärmeübergang aufgestellt. Schließlich wird eine experimentelle Rechtfertigung für das Konzept der in [2] angeführten Grenzschicht gegeben.

ТЕПЛООБМЕН В ПСЕВДООЖИЖЕННЫХ ГАЗОМ СЛОЯХ, ВОЗБУЖДАЕМЫЙ ГАЗОВЫМИ ПУЗЫРЯМИ

Аннотация — Исследовалось влияние прохождения газовых пузырей на теплообмен в псевдоожиженных газом слоях. В качестве датчика теплообмена использовалась платиновая проволока, а неоднородный псевдоожиженный газом слой моделировался единичной непрерывной струей газовых пузырьков в минимально псевдоожиженном слое. Найдено, что в случае низкотемпературных псевдоожиженных газом слоев мелких частиц 90% переноса тепла происходит за счет нестационарной теплопроводности в эмульсионную фазу, а остальные 10% приходятся на газовую конвекцию. Разработана теоретическая модель теплообмена, побуждаемого пузырьками. Наконец, представлено экспериментальное обоснование понятия пограничного слоя свойств, предложенного в работе [2].